Journal of Hydrology (2007) **335**, 170–179

available at www.sciencedirect.com

ScienceDirect

journal homepage: www.elsevier.com/locate/jhydrol

Monin—Obukhov length as a cornerstone of the SEBAL calculations of evapotranspiration

G. Koloskov [a,*], Kh. Mukhamejanov [a], T.W. Tanton [b]

[a] *AIPET, BG Chair of Environmental Technology, Almaty 050013, 126 Baitursynov Street, Kazakhstan*
[b] *University of Southampton, School of Civil Engineering and the Environment, Southampton SO14 7BJ, UK*

Received 27 February 2006; received in revised form 1 October 2006; accepted 20 November 2006

KEYWORDS
SEBAL;
Evaporative fraction;
Monin—Obukhov length;
Evapotranspiration;
Satellite imaging;
Crop water demand;
Water management

Summary The paper looks at the pivotal role that the Monin—Obukhov length (L) can play within the sensible heat balance method for calculating evapotranspiration from remotely sensed multispectral data. It focuses on the possibility of using L as a cornerstone parameter for calculations of sensible heat flux from the pixel data. The paper shows that L can be separated from the other unknowns and can be found either by means of any general one-dimensional root finding method, or iteratively, starting with $L \simeq -\infty$. A simple algorithm is suggested to reduce the number of iterations. The paper goes on to show that all other output parameters can be calculated directly from the value of L that is established, and an analytical expression for the evaporative fraction found.

A novel approach is proposed that allows a close approximation of the evaporative fraction to be derived directly without the need for time-consuming iterations within the main calculation step. Estimates of evapotranspiration from cotton in Southern Kazakhstan showed that the approximation performed well when compared with estimates of $ET_{\mathbf{crop}}$ made using an iterative approach.

An experimental approach for calculating E_{24} is described for use in areas with minimal cloud cover. Comparison of SEBAL estimated Et_c with calculated Et_0 for the short season cotton crop in Southern Kazakhstan indicated that for the actively transpiring cotton crop the crop factors were the same as those determined experimentally for low short season cotton in Kansas by Hunsaker [Hunsaker, D.J., 1999. Basal crop coefficients and water use for early maturity cotton. Trans. ASAE 42(4), 927—936].

Introduction

Increasing population pressure is placing an unsustainable demand on the world's freshwater resources. The large irrigation schemes which produce much of the world's food

* Corresponding author. Tel.: +7 3272 929814.
E-mail addresses: gk-v@yandex.ru (G. Koloskov), twt@soton.ac.uk (T.W. Tanton).

0022-1694/$ - see front matter © 2006 Elsevier B.V. All rights reserved.
doi:10.1016/j.jhydrol.2006.11.010

requirements are by far the biggest consumptive users of water, but are often located in arid climates where water shortage is most acute. It is generally perceived that water use efficiency in most of these schemes is very poor, many being perceived as being less than 40% efficient (Rosegrant, 1997; Heaven et al., 2002) and hence there is an urgent need to establish more effective ways of managing water usage within them. This can only be achieved if water managers have real time knowledge of consumptive evaporative demand throughout schemes rather than user stated demand, or design demand norms. The Penman-Monteith algorithm has been used in conjunction with fairly crude crop and soil moisture correction factors to make estimates of potential crop evapotranspiration (E_t) for planning and design purposes, but the approach is of little practical value for real time scheme management as it relates to ideal agronomic conditions that are rarely achieved in practice. Full reliable data for estimating potential E_t is also often lacking.

Fortunately in recent years algorithms have been developed that allow real time evapotranspiration to be calculated from remotely sensed multispectral data (Bastiaanssen et al., 1998a,b, Bastiaanssen, 1998, 2000, Tasumi et al., 2003, Chemin et al., 2004, Bastiaanssen et al., 2005). The approach uses satellite data to solve the fundamental surface energy balance equation $\lambda E = R_n - G - H$, where the term λE is known as the latent heat flux (W m^{-2}), λ is the latent heat of vaporization (J kg^{-1}), E is the actual evaporation (mm s^{-1}), R_n is the net radiation flux at the surface (W m^{-2}), G is the soil heat flux (W m^{-2}), and H is the sensible heat flux (W m^{-2}). Over a 24 h period soil heat flux will be relatively small and can be ignored while the instantaneous net radiation can fairly readily be obtained from the satellite data. This only leaves the sensible heat flux to be established. The most difficult part of resolving the energy balance equation unfortunately is the separation of the sensible and latent heat fluxes. For unstable atmospheric conditions a number of authors have suggested overcoming the problem by iteratively solving three related unknowns. Jacob et al. (2002) suggested using sensible heat flux (H), Monin–Obukhov length (L) and friction velocity (u_*); (Bastiaanssen, 2000) suggested using H, u_* and aerodynamic resistance for heat transport (r_{ah}); and Bastiaanssen et al. (2005) suggested H, u_* and a temperature scale (T_*). All three iterative approaches are aimed at establishing a convergence on H. They all require the near surface air temperature T_s to be established from the pixel data. This is achieved through a calibration step that requires the establishment of the linear relationship between the surface and air temperature, obtained from selected wet (cold) and a dry (hot) pixel data (Bastiaanssen, 2000).

An interesting attempt to transform the system to one non-linear equation in terms of a special dimensionless variable is demonstrated in Gieske (2003). However the method presented assumes temperature difference δT to be known as a linear function of T_s and hence can not be applied at the calibration step for deriving the most crucial calibration parameters, namely the coefficients of that linear function.

This paper demonstrates that in establishing the surface to air heat loss, although there are small differences in the three approaches, the systems can be converted such that only a single equation with one unknown, namely the Monin–Obukhov length, needs to be solved iteratively. All the other parameters can be derived directly from the value of L found.

An instantaneous estimation of evapotranspiration is of little practical use. If it is assumed that the surface albedo and the evaporative fraction remains effectively constant throughout the day, daily evapotranspiration can readily be established from the calculated instantaneous evaporative fraction and daily net radiation measurements taken from any nearby metrological station equipped with a net radiometer (Bastiaanssen, 2000). Unfortunately in many parts of the world net radiometer data is not readily available. This paper therefore, also proposes an approach for use in arid regions with little cloud for estimating daily evapotranspiration from instantaneous data utilizing the instantaneous evapotranspiration fraction, knowledge of the local solar sun time of image capture, sunrise and sunset times.

The Monin–Obukhov length

Brutsaert (1982) showed that in general under unstable (daytime) conditions the Monin–Obukhov length can be derived from

$$L = -\frac{u_*^3 \rho_a C_P T_a}{g\kappa(H + c_{061} C_P T_a E)} \text{ (m)}, \tag{1}$$

where u_* is the friction velocity (m s^{-1}), ρ_a is the air density (kg m^{-3}), C_P = 1004 (J kg^{-1} K^{-1}) is air specific heat, T_a is the air temperature (K), g is the acceleration due to gravity, κ = 0.4 is the Kármán's constant, H is the sensible heat flux (W m^{-2}) and c_{061} is a constant of 0.61. The actual evaporation E can be derived from the main surface energy balance equation

$$E = \frac{1}{\lambda}(R_n - G - H) \text{ (mm s}^{-1}\text{)}, \tag{2}$$

where R_n is the net radiation flux at the surface (W m^{-2}), G is the soil heat flux (W m^{-2}) and λ is the latent heat of vaporization for water, which can be estimated as a linear function of absolute air temperature T_a (K)

$$\lambda = c_{0_\lambda} - c_{1_\lambda} T_a \text{ (J kg}^{-1}\text{)} \tag{3}$$

with calibration constants $c_{0_\lambda} = 3,148,000$ (J kg^{-1}), $c_{1_\lambda} = 2375$ (J kg^{-1}K^{-1}), derived from Table 3.4 in Brutsaert (1982).

In the calculation of evapotranspiration using the SEBAL (surface energy balance algorithm for land) method, the surface air temperature is obtained by establishing the surface air temperature difference, which can be calculated indirectly using data from extreme 'wet' and 'dry' pixels (Bastiaanssen et al., 1998a). For both of these two extreme pixels L in Eq. (1) can be simplified to:

$$L = -\frac{u_*^3 \rho_a C_P T_a}{g\kappa H} \text{ (m)} \tag{4}$$

for the dry pixel, since $E \simeq 0$ and

$$L = -\frac{u_*^3 \rho_a}{g\kappa c_{061} E} \text{ (m)} \tag{5}$$

for the wet pixel, since $H \simeq 0$.

Calibration step

To establish an energy balance for a given pixel in SEBAL the Monin—Obukhov length L and air temperature difference δT between the two predefined heights z_2 and z_1 must be found (Bastiaanssen et al., 2005). As a linear relationship exists between δT and near surface temperature T_s

$$\delta T = c_{0_{\delta T}} + c_{1_{\delta T}} T_s \text{ (K)}, \tag{6}$$

where $c_{0_{\delta T}}$ and $c_{1_{\delta T}}$ are linear coefficients (Bastiaanssen et al., 2005), the main aim of the calibration step is to derive them from the wet and dry pixels data

$$c_{1_{\delta T}} = \frac{\delta T_{\text{dry}}}{T_{s_{\text{dry}}} - T_{s_{\text{wet}}}}, \quad c_{0_{\delta T}} = -c_{1_{\delta T}} T_{s_{\text{wet}}} \text{ (K)}, \tag{7}$$

where $T_{s_{\text{dry}}}$ is T_s of the dry pixel, $T_{s_{\text{wet}}}$ is T_s of the wet pixel and δT_{dry} is δT of the dry pixel.

Dry pixel

Bastiaanssen, 2000 defined sensible heat flux H as

$$H = \frac{\rho_a c_P}{r_{ah}} \delta T \text{ (W m}^{-2}\text{)}, \tag{8}$$

where δT is the surface-air temperature difference and r_{ah} (s m^{-1}) the aerodynamic resistance to heat transport. If this relationship is combined with Eq. (4), it reveals a simple relationship under dry pixel conditions:

$$-\frac{T_a}{\delta T} = 1 - \frac{T_s}{\delta T} = F_L, \tag{9}$$

where F_L is a dimensionless L-factor representing an aggregation of all L-dependent components and can be defined either as

$$F_L = \frac{g\kappa L}{u_*^3 r_{ah}}, \quad \text{or,} \tag{10}$$

expanding the equations for r_{ah} and u_* (Bastiaanssen, 2000), simply as

$$F_L = gL\frac{L_m^2}{u_x^2 L_h}, \tag{11}$$

where u_x is the wind speed at blending height (m s^{-1}); L_h the stability-corrected logarithmic term for heat transport and L_m the stability-corrected logarithmic term for momentum transport. L_h and L_m are defined as

$$L_h = \ln(z_2/z_1) - \Psi_h(z_2, L) + \Psi_h(z_1, L), \tag{12}$$
$$L_m = \ln(z_x/z_{0m}) - \Psi_m(z_x, L) + \Psi_m(z_{0m}, L), \tag{13}$$

where z_x is the blending height, z_{0m} is the momentum roughness length and Ψ_h and Ψ_m are stability correction functions for heat and for momentum transport respectively. Since the roughness length for momentum transport z_{0m} is not a scalar, it is more natural to rewrite the expression suggested in Bastiaanssen (2000) in an equivalent form

$$z_{0m} = c_{0_{z0m}} \exp(c_{1_{z0m}} \text{SAVI}) \text{ (m)}, \tag{14}$$

where the base height $c_{0_{z0m}} = 0.003$(m), $c_{1_{z0m}} = 5.62$ and SAVI is the soil adjusted vegetation index obtained from satellite data. Caution should be used when using Eq. (14) as it is essential to fine tune the coefficients to the image and local conditions.

The stability correction terms for heat transport Ψ_h and for buoyancy effects on the momentum flux Ψ_m can be expressed as functions of L (Brutsaert, 1982):

$$\Psi_h(z, L) = 2\ln((1 + x^2)/2), \tag{15}$$
$$\Psi_m(z, L) = \ln((1 + x)/2) + \ln((1 + x^2)/2) - 2\arctan(x) + \pi/2, \tag{16}$$

where x is defined as $x = \sqrt[4]{(1 - 16z/L)}$ for unstable (daytime) conditions.

The use of Eq. (9) allows the value of δT for dry pixels to be expressed analytically as a function of L:

$$\delta T = \frac{T_s}{1 - F_L} \text{ (K)}. \tag{17}$$

Unlike the simplicity of the Eq. (17) for deriving δT from known Monin—Obukhov length (L), obtaining L itself is more complicated.

Under conditions of a dry surface it can be assumed that sensible heat flux H to the air can be found as the difference between net radiation flux R_n at the surface and soil heat flux G. L-dependent parameters can be separated from this relationship using the following set of equations:

$$\left.\begin{aligned} &R_n = (1 - \alpha)R_{S\downarrow} - R_{L\uparrow} + \epsilon_s R_{L\downarrow} \text{ (W m}^{-2}\text{)},\\ &R_{L\uparrow} = \epsilon_s \sigma T_s^4 \text{ (W m}^{-2}\text{)},\\ &R_{L\downarrow} = \epsilon_a \sigma T_a^4 \text{ (W m}^{-2}\text{)},\\ &G = G_{fr} R_n \text{ (W m}^{-2}\text{)}, \end{aligned}\right\} \tag{18}$$

where $R_{S\downarrow}$ is the incoming shortwave radiation (W m^{-2}), $R_{L\downarrow}$ is the incoming longwave radiation (W m^{-2}), $R_{L\uparrow}$ is the outgoing longwave radiation (W m^{-2}), α is the surface albedo, ϵ_s is the surface emissivity, ϵ_a is the atmospheric emissivity, $\sigma = 5.67 \times 10^{-8}$(W m^{-2} K^{-4}) is the Stephan—Boltzmann constant, and G_{fr} is the soil heat flux fraction of net radiation, which can be taken either as a simple fraction of R_n (Brutsaert, 1982), or as a sophisticated function of surface temperature, albedo and vegetation index (Bastiaanssen et al., 1998a). What is important is that the G_{fr} does not depend on neither L, nor δT. Thus the expression for H under dry conditions can be expressed as

$$H = c_{0_{R_n}} + c_{1_{R_n}} T_a^4 \text{ (W m}^{-2}\text{)}, \tag{19}$$

where

$$c_{0_{R_n}} \equiv (1 - G_{fr})((1 - \alpha)R_{S\downarrow} - R_{L\uparrow}) \text{ (W m}^{-2}\text{)}, \tag{20}$$
$$c_{1_{R_n}} \equiv (1 - G_{fr})\epsilon_s \epsilon_a \sigma \text{ (W m}^{-2}\text{K}^{-4}\text{)}. \tag{21}$$

These constants do not depend on either L, nor δT and hence, can be precalculated.

It follows from Eq. (9) that for the dry conditions $T_a = -F_L T_s/(1 - F_L)$. In Eq. (4) ρ_a can be expanded as $\rho_a = \frac{\mu P}{R T_a}$, where μ is the air molecular mass 0.029(kg mol^{-1}), R is the gas constant 8.314(J K^{-1} mol^{-1}) and P is the atmospheric pressure (Pa). Replacing H according to Eqs. (19) and (4) can then be rewritten in the form $L = f_d(L)$, where

$$f_d(L) = -\frac{c_{2_{fd}} P}{L_m^3 \left(c_{0_{R_n}} + c_{1_{R_n}} T_s^4 \left(\frac{F_L}{1 - F_L}\right)^4\right)} \text{ (m)}, \tag{22}$$

where $c_{2_{fd}} \equiv \kappa^2 u_x^3 \mu c_P/(gR)$ (W m^{-1} Pa^{-1}).

Expressing the atmospheric pressure P as

$$P = P_0\left(1 - \frac{c_{0_P}}{T_a} z\right)^{c_{1_P}} \text{ (Pa)}, \tag{23}$$

where P_0 is the atmospheric pressure at sea level 101,300 (Pa), z is the elevation above sea level (m), and calibration constants c_{0_P} and c_{1_P} are 0.0065 (K m^{-1}) and 5.26 respectively, a simple solution is given by assuming $P(T_a) \simeq P(T_0)$, where $T_0 = 293$ (K) is the standard temperature. This gives a constant value of P for the whole image. Alternatively T_a can be expressed in terms of T_s and F_L in which case Eq. (23) transforms into

$$P = P_0\left(1 + c_{0_P} \frac{1 - F_L}{F_L T_s} z\right)^{c_{1_P}} \text{ (Pa)}. \tag{24}$$

In any case the right-hand side of Eq. (22) is L-dependent only. The solution of the non-linear equation $f_d(L) - L = 0$, which can be done using any general root finding method, gives the last parameter needed to derive, the Monin—Obukhov length L. It can also be derived iteratively using Eq. (22) starting with $L \simeq -\infty$, until the desired accuracy is reached.

Unrestricted soil moisture conditions

A wet analogue of Eq. (11) can be obtained from Eq. (5):

$$L = f_w(L) \text{ (m)}, \quad f_w(L) = -\frac{c_{0_{fw}}}{L_m^3} \text{ (m)}; \tag{25}$$

$$c_{0_{fw}} \equiv \frac{\kappa^2 u_x^3 \rho_a \lambda}{c_{061} g (R_n - G)} \text{ (m)}. \tag{26}$$

Main calculations (mixed conditions)

With known constants (for the satellite image in question) $c_{0_{\delta T}}$ and $c_{1_{\delta T}}$, obtained from Eq. (7), parameter δT for all the other pixels can be calculated from surface temperature T_s using Eq. (6).

Iterative solution

As Bastiaanssen et al. (2005) recently pointed out, the stability correction functions Ψ_h and Ψ_m have to be calculated iteratively for every pixel to derive the Monin—Obukhov length for each.

The equivalent of Eqs. (22) and (25) suitable for calculation of the Monin—Obukhov length for any pixel under mixed conditions is therefore $L = f_m(L)$, where

$$f_m(L) = -\frac{c_{2_{fm}} u_x^2 L_h}{g L_m^2 (c_{0_{fm}} + c_{1_{fm}} L_m L_h)} \text{ (m)}. \tag{27}$$

The coefficients

$$c_{0_{fm}} \equiv \delta T(\lambda - c_{061} C_P T_a) \text{ (J kg}^{-1}\text{ K)}, \tag{28}$$

$$c_{1_{fm}} \equiv c_{061} T_a (R_n - G)/(\kappa^2 u_x \rho_a) \text{ (J kg}^{-1}\text{ K)}, \tag{29}$$

$$c_{2_{fm}} \equiv T_a \lambda \text{ (J kg}^{-1}\text{ K)} \tag{30}$$

need only be calculated once from pixel data, since they are not dependent on L and are constant for any particular pixel within the image, L_h and L_m are calculated the same way as in Eqs. (12) and (13). Eq. (27) can be solved in much the same way as Eq. (22), hence values of sensible and latent heat fluxes can be calculated for every pixel. A direct approximation approach as described later in this paper can however help avoid time-consuming iterations.

Heuristic for the rapid calculation of L

The heuristic for speeding up convergence of the iterative process is general for all three cases: wet, dry and mixed pixel calculations. It exploits the fact that plotting values of $\ln(-f(L)) - \ln(-L)$ against $\ln(-L)$ gives curves that are almost straight lines from $L = -\infty$ to the point of interest, where the curves intercept zero (see Fig. 1). Thus the function can be assumed approximately linear in the local region of interest, hence the secant method (Press et al., 1992), that converges more rapidly near a root of such a sufficiently continuous function, can be effectively used.

The algorithm starts with obtaining two initial points on the curve, (a,c) and (b,d):

$$\left.\begin{array}{ll} L_0 = -1000; & f_0 = f(L_0); \\ a = \ln(-L_0); & c = \ln(-f_0) - a; \\ L_1 = f_0; & f_1 = f(L_1); \\ b = \ln(-L_1); & d = \ln(-f_1) - b. \end{array}\right\} \tag{31}$$

At this point function $f(L)$ is calculated twice and the algorithm is then ready for the next step $k = 2$ (here $f(L)$ means $f_d(L)$, $f_w(L)$ and $f_m(L)$ for dry, wet and mixed pixels, respectively). From here on all the following values of L_k are

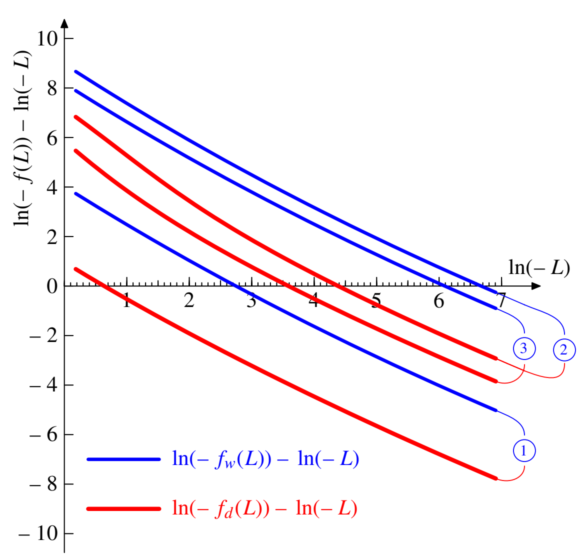

Figure 1 Plots of functions, used to obtain Monin—Obukhov length for wet and dry calibration pixels for the three images: (1) 10/08/2002, (2) 28/07/2003 and (3) 30/09/2003. The zero points correspond to the following values of L(m):

Date	10/08/2002	28/07/2003	30/09/2003
Dry	−1.892	−80.222	−36.185
Wet	−15.600	−789.946	−444.244

derived from linear approximation of the value of L, where the line (a,c)—(b,d) intercepts zero:

$$t = \frac{ad - bc}{d - c}; \quad L_k = -\exp(t); \quad f_k = f(L_k) \tag{32}$$

and the points are adjusted for the next step: $a = b$; $c = d$; $b = t$; and $d = \ln(-f_k) - b$.

Thus while every step costs only one calculation of the 'heavy' function $f(L)$ as in the simple iterative solution, plus some extra simple calculations, such an approach gives a noticeable reduction in computational time, being almost twice as fast as the iterative approach. The technique was found to achieve an accuracy of $L \pm 5 \times 10^{-5}$ m in about 4—6 steps.

Separation of the sensible and the latent heat fluxes

With values of L and δT obtained, the sensible and latent heat fluxes can conveniently be separated by expressing their appropriate fractions analytically as functions of L and δT (T_s, in fact).

A combination of Eqs. (1), (2), (8) and (10) helps to express the aerodynamic resistance term to heat transport r_{ah}, the only L-dependent parameter needed to separate H from E, in terms of the L-dependent parameter F_L as:

$$r_{ah} = \frac{\rho_a C_P}{R_n - G}\left(\delta T - \left(\frac{\delta T}{T_a} + \frac{1}{F_L}\right)\frac{\lambda}{c_{061} C_P}\right) \ (\mathrm{s\ m^{-1}}), \tag{33}$$

thus the value of sensible heat flux for a pixel can then be found as a fraction of ($R_n - G$):

$$H = H_{fr}(R_n - G) \ (\mathrm{W\ m^{-2}}), \tag{34}$$

where H-fraction H_{fr} is defined as

$$H_{fr} = \frac{\delta T}{\delta T - \left(\frac{\delta T}{T_a} + \frac{1}{F_L}\right)\frac{\lambda}{c_{061} C_P}}. \tag{35}$$

Similarly

$$E = \frac{E_{fr}}{\lambda}(R_n - G) \quad (\mathrm{mm\ s^{-1}}), \tag{36}$$

where E-fraction E_{fr} is defined as

$$E_{fr} = \frac{\left(\frac{\delta T}{T_a} + \frac{1}{F_L}\right)}{\left(\frac{\delta T}{T_a} + \frac{1}{F_L}\right) - \frac{c_{061} C_P}{\lambda}\delta T}. \tag{37}$$

Direct approximation of the sensible and latent heat fluxes

A temperature-ruled evaporative fraction (TREF) model is suggested as an alternative approach to avoid the iterative solution of L for every pixel. It is based on the assumption that the relationship between δT and L in Eq. (9) for the dry conditions is only a special case of a more general linear relationship

$$T_s/(1 - F_L) = c_{0_{F_L}} + c_{1_{F_L}}\delta T \ (\mathrm{K}), \tag{38}$$

where $c_{0_{F_L}}$ and $c_{1_{F_L}}$ are constants for the satellite image in question. The data obtained at the calibration step can be used to establish that

$$c_{0_{F_L}} = \frac{T_{s_{wet}}}{1 - F_{L_{wet}}} \ (\mathrm{K}) \quad \text{and} \quad c_{1_{F_L}} = 1 - \frac{c_{0_{F_L}}}{\delta T_{dry}}, \tag{39}$$

where $F_{L_{wet}}$ is the F_L of the wet pixel. Such linearization leads to an interesting outcome: approximated values of E_{fr} (usually the most important aim of the calculations) for a general pixel can be obtained without a need to iteratively find the value of the Monin—Obukhov length. The only two 'heavy' iterative calculations of L that are then necessary are for the wet and for the dry pixel at the calibration step.

If Eq. (38) is used to linearise Eqs. (34)—(37), this directly gives an approximate value of F_L for any pixel as

$$F_L = 1 - \frac{T_s}{c_{0_{F_L}} + c_{1_{F_L}}\delta T}. \tag{40}$$

The key parameters δT and the Monin—Obukhov length L that were determined from the wet and dry pixels at the calibration step are used to anchor the latent and sensible heat flux fractions. It is interesting to note that the latent and sensible heat fractions are directly related to the surface temperature of the pixel since all the other parameters (δT, T_a and λ) are in fact a linear functions of T_s. Another interesting feature of such a method is that an average wind speed parameter u_x is not shown in the final equations for H and E: rather its influence is hidden deeply in the values of parameters $c_{0_{\delta T}}$, $c_{1_{\delta T}}$ and $c_{0_{F_L}}$, $c_{1_{F_L}}$, obtained at the calibration step.

Estimation of the daily evapotranspiration

Irrespective of the way in which the value of F_L was obtained — iteratively or by approximation (40), expression (36) provides an instantaneous value of E (mm s^{-1}), which can be expanded to an hourly interval as $E_h = c_{hour}E$ (mm h^{-1}), where $c_{hour} = 3600$ (s h^{-1}).

Bastiaanssen et al. (2005) computed daily evapotranspiration from the instantaneous evaporative fraction, defined as

$$E_{fr} = \frac{\lambda E}{R_n - G}. \tag{41}$$

In practice over a 24-h period G can be ignored, and if surface albedo throughout the day is assumed to be the same as the morning overpass the evaporative fraction throughout the day can be assumed to be constant. Hence daily evapotranspiration is given by

$$E_{24} = c_{day}\frac{E_{fr}R_{n_{24}}}{\lambda} \ (\mathrm{mm\ d^{-1}}), \tag{42}$$

where $R_{n_{24}}$ (W m^{-2}) is the daily average net radiation, $c_{day} = 86{,}400$ (s d^{-1}). From a procedure suggested by Slob (de Bruin, 1987),

$$R_{n_{24}} = (1 - \alpha)K_{24} - 110\tau_{sw_{24}} \ (\mathrm{W\ m^{-2}}), \tag{43}$$

where K_{24} (W m^{-2}) is the daily average solar radiation and $\tau_{sw_{24}}$ is the daily atmospheric transmittance, determined from instrumentation in the field.

Although this approach is sound there are few irrigation projects that have field instrumentation to measure solar radiation directly. The approach outlined below gives a method that for arid climates with little cloud cover was found to give a reliable estimate of daily evapotranspiration in Southern Kazakhstan. It is based on the assumption that incoming radiation and the daily evapotranspiration curves are close to a parabola (Fig. 2) with a maximum close to noon, and the time between zero points close to the daylight hours:

$$E_{\mathrm{h}}(t) \simeq \frac{(c_{\mathrm{es}}\tau_{\mathrm{sun}})^2 - 4(t-12)^2}{(c_{\mathrm{es}}\tau_{\mathrm{sun}})^2 - 4(t_{\mathrm{img}}-12)^2} E_{\mathrm{h_{img}}} \ (\mathrm{mm\ h^{-1}}), \tag{44}$$

where E_{h} (mm h^{-1}) is the hourly evaporation as a function of time, $E_{\mathrm{h_{img}}}$ (mm h^{-1}) is the hourly evaporation, calculated from the image pixel data, t (h) is the timescale, τ_{sun} (h) is the daylight period, t_{img} (h) is the image acquisition time

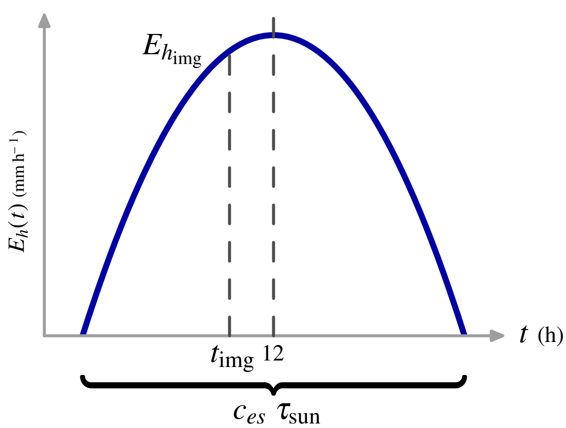

Figure 2 Approximation of daily evaporation.

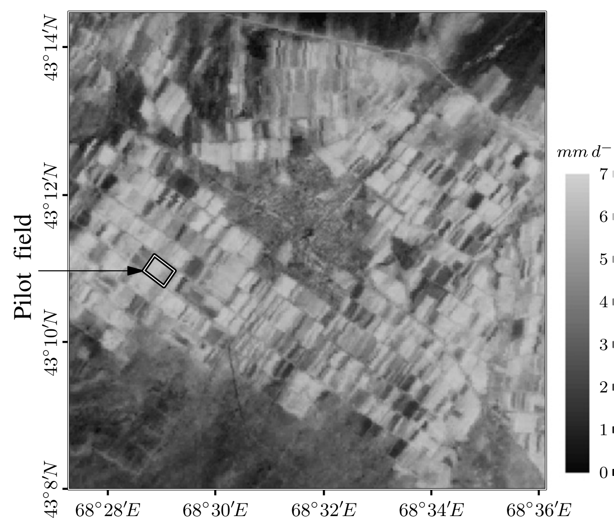

Figure 3 Spatial distribution of E_{24} in 12 × 12 km area on 10/08/2002.

Table 1 Parameters for the wet and the dry pixels, calculated at the calibration step for three Landsat7 satellite images

		10/08/2002		28/07/2003		30/09/2003	
		Dry	Wet	Dry	Wet	Dry	Wet
θ	rad	0.596		0.547		0.859	
u_x	(m s^{-1})	2.693		12.700		9.839	
τ_{sw}	—	0.754		0.754		0.754	
α	—	0.285	0.208	0.265	0.198	0.269	0.200
SAVI	—	0.157	0.419	0.363	0.507	0.148	0.439
LAI	—	0.112	0.859	0.652	1.294	0.093	0.946
$z_{0\mathrm{m}}$	m	0.007	0.032	0.023	0.052	0.007	0.035
ϵ_{a}	—	0.759		0.759		0.759	
ϵ_{s}	—	0.951	0.959	0.957	0.963	0.951	0.959
T_{s}	K	319.721	301.484	308.148	293.932	303.423	291.305
T_{a}	K	314.454	301.484	304.688	293.932	299.917	291.305
δT	K	5.266	0.0	3.460	0.0	3.507	0.0
$R_{S\downarrow}$	W m^{-2}	831.378		854.524		673.348	
$R_{L\downarrow}$	W m^{-2}	420.510	355.307	370.652	321.019	347.975	309.697
$R_{L\uparrow}$	W m^{-2}	563.506	449.030	489.010	407.539	457.013	391.744
R_{n}	W m^{-2}	430.679	550.014	493.292	587.146	365.919	444.007
G_{fr}	—	0.275	0.147	0.198	0.102	0.175	0.092
G	W m^{-2}	118.457	80.668	97.783	60.037	64.117	40.991
H	W m^{-2}	312.222	0.0	395.510	0.0	301.802	0.0
H_{fr}	—	1.0	0.0	1.0	0.0	1.0	0.0
E_{fr}	—	0.0	1.0	0.0	1.0	0.0	1.0
E_{h}	mm h^{-1}	0.0	0.695	0.0	0.8	0.0	0.591
E_{24}	mm h^{-1}	0.0	6.452	0.0	7.414	0.0	4.685
L	m	−1.892	−15.600	−80.222	−789.946	−36.185	−444.244
L_{h}	—	1.402	2.411	2.831	2.977	2.676	2.962
L_{m}	—	5.716	5.831	7.144	7.229	7.896	7.448
F_L	—	−59.713	−298.016	−88.049	−844.231	−85.529	−843.769

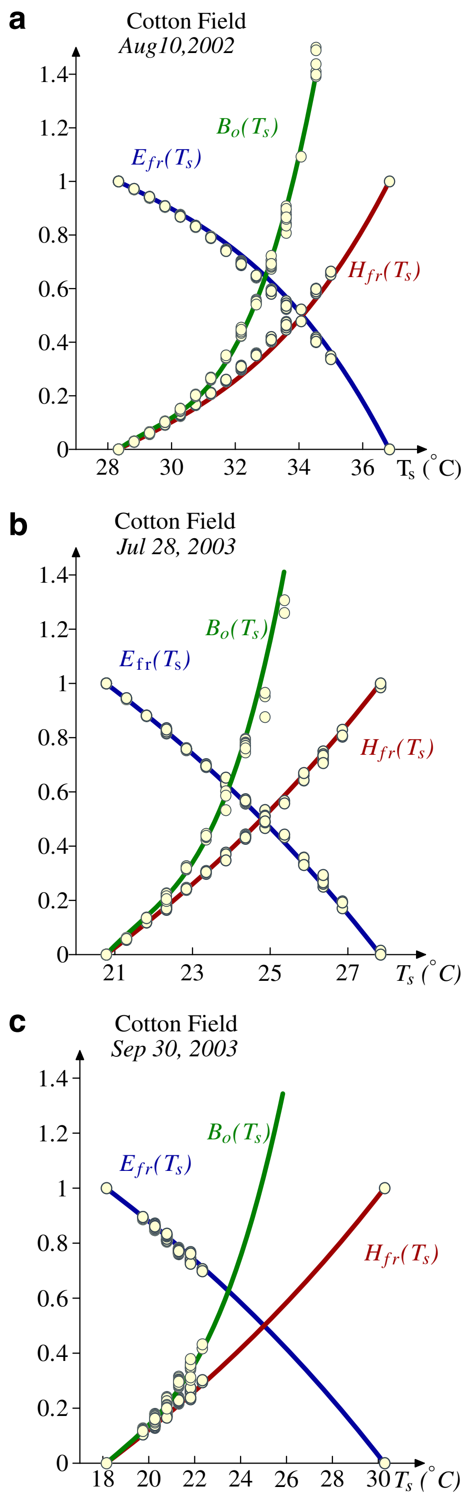

Figure 4 Comparison of the estimates of evaporative fraction E_{fr}, sensible heat fraction H_{fr} and Bowen ratio B_o calculated using iteratively derived L from Eq. (27) (symbols) with those derived from the approximation of F_L using Eq. (40) (solid lines).

(converted to local sun time), and c_{es} is a calibration constant 0.93.

In which case daily evapotranspiration E_{24} can be approximated as:

$$E_{24} \simeq \int_{12-\frac{c_{es}\tau_{sun}}{2}}^{12+\frac{c_{es}\tau_{sun}}{2}} E(t)\,dt \ (\mathrm{mm\ d^{-1}}), \tag{45}$$

thus

$$E_{24} \simeq \frac{2}{3}\frac{E_h(c_{es}\tau_{sun})^3}{(c_{es}\tau_{sun})^2 - 4(t_{img}-12)^2} \ (\mathrm{mm\ d^{-1}}). \tag{46}$$

Validation at pilot field scale

Validation of the methodology was carried out on the very large Arys-Bugun irrigation project in the hot dry steppe of Southern Kazakhstan, 43°11′N, 68°29′E. Cotton dominates the scheme, being grown in blocks of about 30—50 ha. The climatologically instrumented cotton field used to validate the methodology was sited near Turkestan and was covered by approximately 300 Landsat 7 pixels. The field had a good stand of short season cotton and at maturity in August a fully developed canopy. The crop was typically about 70—80 cm high cotton. The potential evapotranspiration of cotton ($E_{t\ cotton}$) was calculated from the infield climate data and Hunsaker's (1999) short season cotton crop coefficients. The validation on a wider scale was carried out within a 144 km^2 area centered on Staroikan village, comprising approximately 8 km^2 village, 100 km^2 of irrigation (active and abandoned) and 36 km^2 of steppe (see Fig. 3). The remotely sensed data was from Landsat 7 images gathered on cloud free days on 10/08/2002, 28/07/2003 and 30/09/2003.

The output data for the experimental field calibration step for the three images is given in Table 1.

Fig. 4a—c show for the three data sets how the evaporative fraction (E_{fr}), sensible heat fraction (H_{fr}) and Bowen ratio (B_o) relate to surface temperature assuming the simultaneous presence of wet and dry areas, and illustrate the good correlation that exists between the complete iterative and approximated direct approaches. The ends of the the E_{fr} and H_{fr} curves are fixed by the extreme cold (recently irrigated cotton field) and hot (dry vegetation in un-irrigated field) pixel data. The advantage of the direct approximation approach Eq. (40) over Eq. (37) is that it allows the relationship to be calculated over the whole temperature range of interest.

Validation at the regional scale

Distribution of the number of iterations (using the rapid heuristic approach) used to derive L with an accuracy of $\pm 5\times10^{-5}$ m for the 144 km^2 study area is summarized in

Table 2 Relationship between the number of iteration steps and the frequency of obtaining an accuracy better than $\pm 5\times10^{-5}$ m for L

Iterations	10/08/2002	28/07/2003	30/09/2003
3	0.01%		
4	1.07%	8.68%	7.05%
5	97.42%	91.32%	92.95%
6	1.50%		

Table 3 Comparison between estimates of evapotranspiration in an area of 144 km^2 made by the iterative (E_{24_i}) and approximation (E_{24_a}) methods

Image date	E_{24_i}		E_{24_a}		Δ_{ia}	
	Mean	SD	Mean	SD	Mean	SD
10/08/2002	3.92	1.49	4.14	1.33	−0.22	0.18
28/07/2003	3.15	2.01	3.08	2.01	0.07	0.15
30/09/2003	2.13	1.35	2.18	1.35	−0.04	0.07

Table 2. For the majority of pixels (>98%) no more than five iterations were needed to derive an accurate value of L.

Direct comparison of pixel distributions of the daily evaporation calculated by the iterative and approximated direct methods can be seen in Table 3 and Fig. 5a—c. The

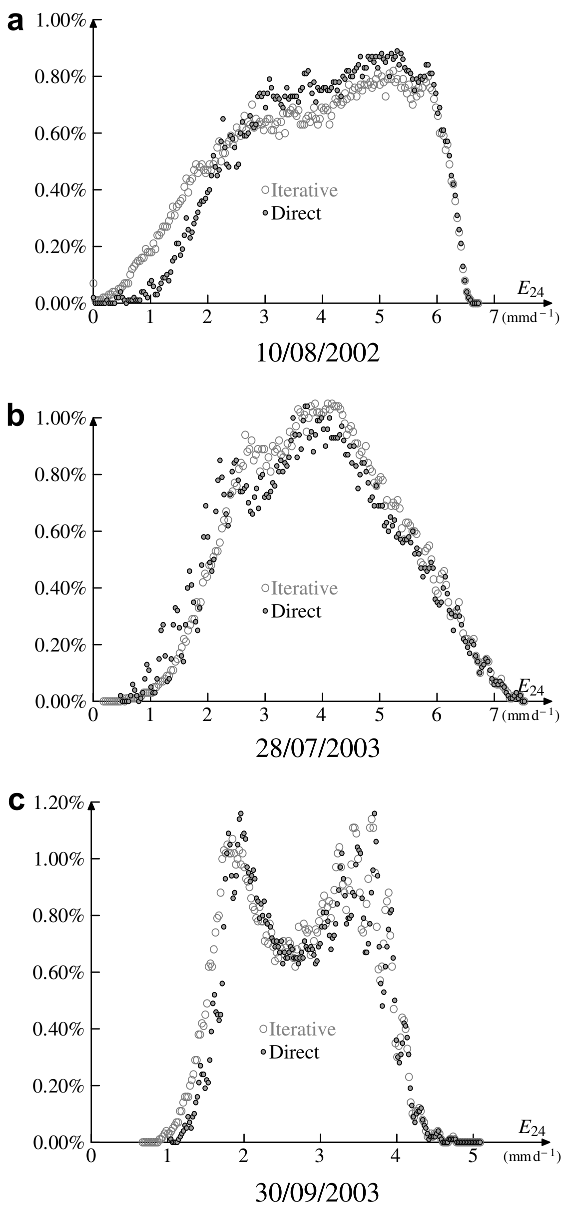

Figure 5 The pixel distribution of calculated E_{24} (mm d^{-1}) using accurate iterative and approximated direct approach, Arys-Bugun irrigation project in Southern Kazakhstan, 12 × 12 km fragment.

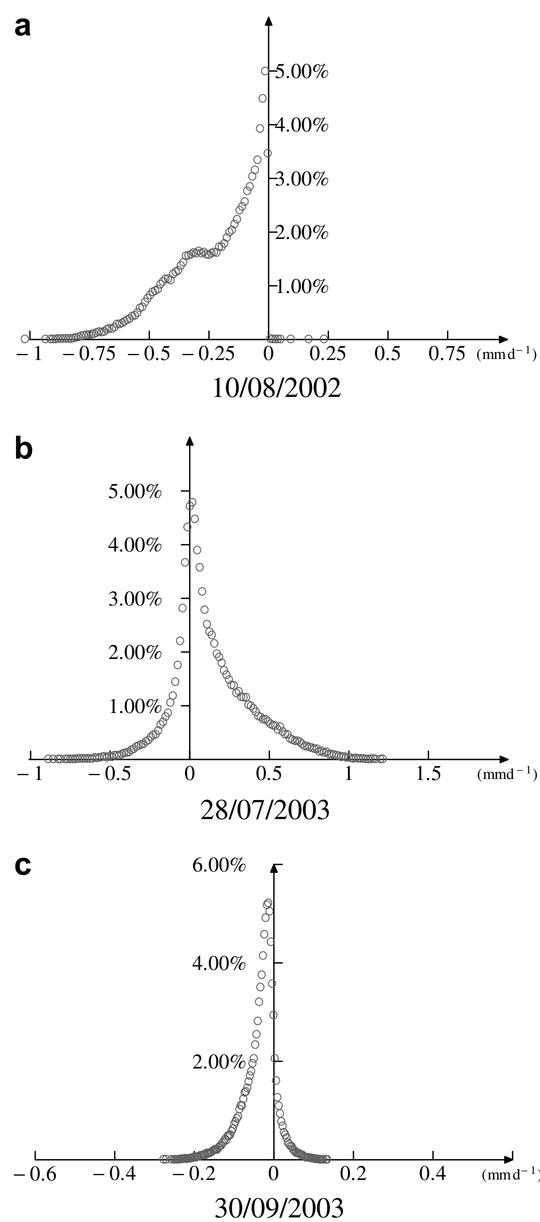

Figure 6 The distribution of differences between iterative and linearized approaches in estimating E_{24} (mm d^{-1}).

Table 4 Comparison of SEBAL estimates of evapotranspiration

Date	Et_{inst}	Et_0	Et_{24}		K_c	
	mm/h		mm/d			
	SEBAL	Penman	SEBAL	Penman	SEBAL	Hunsaker
10/08/2002	0.64	0.56	5.94	5.63	1.06	1.10
28/07/2003	0.68	0.64	6.53	7.27	0.90	0.90
30/09/2003	0.41	0.54	3.48	4.78	0.73	0.40

distribution of the pixel differences between these two approaches is shown in Fig. 6.

Discussion and conclusions

The paper clearly demonstrates the pivotal role that the Monin—Obukhov length plays in taking account of turbulent heat exchange and the convective process to establish evapotranspiration from remotely sensed data.

A new suggested dimensionless parameter F_L, that ties together all L-dependant parameters together, can be approximated directly for any pixel by the simple relationship given in Eq. (40) using two additional parameters derived at a calibration step. The price of such an approach is that the value of L and hence, u_* remains unknown. This is not a problem however, since the aim is to establish the evaporative fraction, which can be efficiently derived via the approximation approach.

Comparison of the iterative (Bastiaanssen et al., 2005) and direct approximation approaches for establishing the sensible and latent heat fluxes from Lansat 7 data for large irrigated cotton fields in Southern Kazakhstan (Table 3) indicated that the mean differences were small and relatively insignificant (a mean difference in Et_{crop} of 3.5%). This strong agreement indicates that the computationally more efficient approximation approach provides an effective solution for establishing evapotranspiration. There is however a need to test the approach more widely under different climatic and crop conditions to ensure that the technique is widely applicable.

The use of Eq. (46) to estimate daily evapotranspiration from the instantaneous value was highly effective for cotton in the relatively cloud free climate of southern Kazakhstan (Table 4), and is likely to prove a useful technique for deriving daily evapotranspiration in arid regions where cloud cover is sparse and daily net radiation measurement absent.

The crop factors for the fully developed, well irrigated cotton crop established using the temperature-ruled evaporative fraction (TREF) model (Table 4) were lower than the value of 1.2 normally suggested in the literature (e.g. Allen and Pereira, 1998), but were effectively the same as those predicted from the infield climate data using the method developed by Hunsaker (1999) for short season cotton in Kansas. This is not surprising given the lower stature of the short season cotton crop compared to the more usual 1.2 + m crop height found in many parts of the world. This close match supports the use of this model. Estimates of daily evaporation from the dry steppe was very low (typically <0.3 mm d^{-1}). Since the approach also gives an estimate of evapotranspiration for well irrigated cotton very close to that predicted estimates using the Penman Montieth approach (short season cotton K_c), it suggests that the computed temperature range is giving a realistic evaporative scale. In July and August our estimates of daily $E_{t\ cotton}$ growing in the recently irrigated experimental field were very close to cotton's predicted evaporative potential, but our estimate was lower at the end of September. This latter observation was not surprising as irrigation had long since ceased to speed bole development and ripening to ensure the harvest would be completed before the onset of winter sometime in October.

The cotton fields and irrigation projects of the study area in Southern Kazakhstan are large and almost mono-cropped with cotton. They provide the ideal proving ground for the effectiveness of the sensible energy balance approach to estimating evapotranspiration. Although the proposed approach appears to have worked well under these conditions there is clearly a need to prove its validity under a wider range cropping patterns and climatic conditions.

Acknowledgements

The authors thank European Union and BG Foundation for funding this work. We are also grateful to the anonymous reviewers for their helpful comments and suggestions.

References

Allen, R.G., Pereira, L.S., Raes D., Smith M., 1998. FAO Irrigation and Drainage Paper No. 56 Crop Evapotranspiration. Pub. FAO.

Bastiaanssen, W.G.M., 1998. Remote Sensing in Water Resources Management: The State of the Art. International Water Management Institute, Colombo, Sri Lanka.

Bastiaanssen, W.G.M., 2000. SEBAL-based sensible and latent heat fluxes in the irrigated Gediz basin, Turkey. J. Hydrol. 229, 87—100.

Bastiaanssen, W.G.M., Menenti, M., Feddes, R.A., Holtslag, A.A.M., 1998a. A remote sensing surface energy balance algorithm for land (SEBAL). 1. Formulation. J. Hydrol. 212—213, 198—212.

Bastiaanssen, W.G.M., Noordman, E.J.M., Pelgrum, H., Davids, G., Thoreson, B.P., Allen, R.G., 2005. SEBAL model with remotely sensed data to improve Water-Resources Management under actual field conditions. J. Irrig. Drainage Eng. 131 (1), 85—92.

Bastiaanssen, W.G.M., Pelgrum, H., Wang, J., Ma, Y., Moreno, J.F., Roerink, G.J., van der Wal, T.A., 1998b. A remote sensing surface energy balance algorithm for land (SEBAL). 2. Validation. J. Hydrol. 213, 213—229.

de Bruin, H.A.R., 1987. From Penman to Makkink. In: Hooghart, J.C. (Ed.), Evaporation and Weather. Proceedings and Infor-

mation: TNO Committee on Hydrological Research vol. 39, pp. 5—33.
Brutsaert, W., 1982. Evaporation into the Atmosphere, Theory, History and Applications. Reidel, Dordrecht, The Netherlands.
Chemin, Y., Platonov, A., Ul-Hassan, M., Abdullaev, I., 2004. Using remote sensing data for water depletion assessment at administrative and irrigation-system levels: case study of the Ferghana Province of Uzbekistan. Agric. Water Manag. 64 (3), 183—196.
Gieske, A., 2003. The iterative flux-profile method for remote sensing applications. Int. J. Remote Sensing 24 (16), 3291—3310.
Heaven, S., Koloskov, G.B., Lock, A.C., Tanton, T.W., 2002. Water resources management in the Aral basin: A river basin management model for the Syr Darya. Irrig. Drainage 51 (2), 109—118.
Hunsaker, D.J., 1999. Basal crop coecients and water use for early maturity cotton. Trans. ASAE 42 (4), 927—936.
Jacob, F., Olioso, A., Gu, X.F., Su, Z., Seguin, B., 2002. Mapping surface fluxes using airborne visible, near infrared, thermal infrared remote sensing data and a spatialized surface energy balance model. Agronomie 22, 669—680.
Press, W.H., Teukolsk, S.A., Vetterling, W.T., Flannery, B.P., 1992. Numerical Recipes in C: The Art of Scientific Computing. Cambridge University Press.
Rosegrant, M.W., 1997. Water resources in the 21st century: challenges and implications for action. Food, Agriculture, and the Environment. Discussion Paper 20. Washington, DC: International Food Policy Research Institute.
Tasumi, M., Trezza, R., Allen, R.G., Wright, J.L., 2003. US validation tests on the SEBAL model for evapotranspiration via satellite. In: US Validation Tests on the SEBAL Model for Evapotranspiration via Satellite. ICID Workshop on Remote Sensing of ET for Large Regions, 17 September 2003.